Article:
Istkhar, T., Hafeez, A., Javed, F. et al. (5 more authors) (2023) Intensification of esterification reaction microbubble mediated reactive distillation. Chemical Engineering and Processing - Process Intensification, 191. 109435. ISSN: 0255-2701

https://doi.org/10.1016/j.cep.2023.109435

Chemical Engineering & Processing: Process Intensification 191 (2023) 109435

Contents lists available at ScienceDirect

Chemical Engineering and Processing - Process Intensification

journal homepage: www.elsevier.com/locate/cep

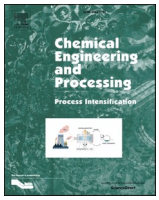

Intensification of esterification reaction microbubble mediated reactive distillation

Talha Istkhar [a], Ainy Hafeez [a], Fahad Javed [a], Tahir Fazal [a,b], Faisal Ahmad [c], Arif Hussain [c], William B.J. Zimmerman [d], Fahad Rehman [a,e,*]

[a] Microfluidics Research Group, Department of Chemical Engineering, COMSATS University, Lahore Campus, Pakistan
[b] Department of Chemical Engineering, Khawaja Fareed University of Engineering and Information Technology, Rahim Yar Khan, Pakistan
[c] Process System Engineering Research Group, COMSATS University Islamabad, Lahore Campus, Pakistan
[d] Department of Chemical and Biological Engineering, The University of Sheffield, UK.
[e] School of Mathematics and Statistics, The Univeristy of Sheffield, UK

ARTICLE INFO

Keywords:
Acid catalysis
Esterification
Methyl acetate
Mass transfer
Microbubbles

ABSTRACT

The current study is based on the microbubble mediated reactive distillation by converting conventional homogeneous liquid-liquid system into a heterogeneous vapour-liquid system. Microbubbles owing to their higher surface area to volume ratio provides better mass transfer as well increasing the conversion and rate of reaction. To prove the hypothesis, production of methyl acetate was investigated because of its industrial importance. The experimental plan was designed using Response Surface Methodology (RSM). It allowed analysing the effects of operational parameters simultaneously. The kinetics investigation demonstrated that the esterification reaction occurs, indeed, on the vapour liquid interface at the skin/surface of the bubble and follows pseudo-first order kinetics. The maximum conversion of the process was found to be 91% in 20 min which is significantly higher than any previous study. Furthermore, RSM and Gated Recurrent Unit (GRU) were employed to develop models to analyse the correlations among parameters and to predict the responses. The GRU produced higher R^2 = 0.9981 as compared to R^2 = 0.9715 produced by RSM. The results depict that GRU model is more robust and reliable than Response Surface Methodology for parameter interaction study and response prediction.

1. Introduction

Esterification is one of the most important reactions in chemical synthesis. It has several numerous industrial application such as biodiesel, pesticides, cosmetics, paints and dyes etc., [1]. Esterification reaction has a low conversion and a low reaction rate and requires an acid catalyst to increase the reaction rate [2]. The low conversion and reaction rate is caused by establishment of equilibrium and poor mass transfer between the reactants [3]. Consequently, the separation of product becomes energy intensive and the overall cost of the process is increased [4]. For instance, the cost for the separation of the product in a distillation column is US$ 0.1345 Million/ton is very high as compare to the cost of catalyst or cost to maintain temperature and pressure [5]. The cost of the separation of the product for different process is given in supplementary data Table S-I.

To overcome the establishment of equilibrium, several methods have been investigated. Esterification process was carried out in reactive distillation (RD) columns in which reaction and separation occur simultaneously [6]. Initially RD was commercially used for the production of methyl acetate in 1983 by Eastman company [7]. The main challenges of the RD are; handling of large size of distillation columns, and low conversion [8]. As the reaction and separation process occur in the same unit due to this azeotropes form in the column and also it increases the design complexity and handling in reactive distillation column [9]. Pressure swing distillation has also been employed for MeOH production. It is carried out in two stages. The column is operated at atmospheric pressure. The esterification reaction is carried out in liquid phase. However, the presence of acetic acid (AcOH), water, methanol and acetate creates adverse equilibrium conditions and consequently reduce the production and purity of the product [10]. Then two column system was purposed-one column for rectifying and the other for the stripping section. However, to increase the purity (%) to 99.5%, a third column had to be introduced [11]. Reactive distillation with divided wall column has been reported for esterification. The reactants were fed

* Corresponding author.
E-mail address: frehman@cuilahore.edu.pk (F. Rehman).

https://doi.org/10.1016/j.cep.2023.109435
Received 14 February 2023; Received in revised form 10 May 2023; Accepted 20 May 2023
Available online 21 May 2023

through the reboiler. The major drawback of this technique was the recovery of the product that was less than 75% [12].

In the current study to overcome current challenges, modified RD system is introduced to conduct reaction in gas-liquid system instead of conventional liquid-liquid system. In conventional system reaction occur in both vapour and liquid phase but large amount of reactants reacts in liquid phase due to this, it is assumed that conventional reaction occurs in liquid phase. In the current system, reactants are introduced in the form of vapours to overcome the mass transfer limitation [6,13] one of the reactants (alcohol) is injected in vapour phase in the form of bubbles [14]. To ensure the generation of microbubbles certain conditions are provided such as, significantly low flow rates and highly porous sintered borosilicate glass diffuser [15,16]. The microbubbles have high surface to volume ratio and interfacial area that increases the rate of reaction and mass transfer rate. Alcohol is fed in the form of vapours. When bubbles enter the reactor they are surrounded with excess amount of carboxylic acid. A high concentration gradient between AcOH (bulk) and alcohol (small bubble) allows the reaction to occur instantaneously and shifts the reaction in forward direction as prescribed by Le Chatelier's [17]. The product flux shifts toward the centre point of the microbubble and, if, the reaction is controlled by the surface of the bubble [18]. The microbubble containing alcohol vapour would rise and keep on reacting with the ``fresh'' carboxylic acid molecule around it. Simultaneously the product flux would keep on increasing towards the centre of the bubble [19].

The bubble would reach the surface and burst. If the boiling point of the product is higher, such as Biodiesel, than the reaction temperature, the product would not leave the system [14], however the unreacted alcohol would leave the system limiting the establishment of equilibrium. If the boiling point of the product is less than reaction temperature, such as acetates, the product would leave the reactor and will be collected in the condenser [19]. Since, the product has left the reactor, equilibrium would be shifted in forward direction.

The reaction, in the conventional MeOH system, occurs mostly in the liquid bulk as compared with gas-liquid system where the reaction occur on surface of the bubble. In conventional system, both the reactants are highly immiscible due to which diffusion of reactants also decreases as a result low rate of reaction and achieved equilibrium at low concentration. However, the amount of alcohol is not present in bulk in the reactor in the form of bubbles at any point in time to establish the equilibrium hence pushing the reaction towards completion. Counter intuitively, the amount of alcohol present in a bubble is always in excess locally as compared to the carboxylic acid at bubble interface-which pushes the equilibrium in the forward the direction. To conclude, alcohol is not present in the bulk to establish equilibrium but is in excess locally in the bubble to react instantaneously with the carboxylic acid present at the interface.

The above explained dynamics of vapour-liquid system is heavily dependent on the size of the bubbles. There are several factors affecting the size of the bubbles. Low flow rates, such as used in the current study tends to produce smaller bubbles in the range of microbubbles [14,15,19]. The other important factor controlling the size of the bubble is the nature of the diffuser used to generate bubble. The reactant (AcOH)--philic diffusers tend to generate microbubbles as the facilitate bubble formation mechanism [15] as shown in Fig 1. The reactant philic mean that if reactant is polar like acetic acid so the diffuser which have polar nature will help to generate microbubble and if the reactant is non polar nature like oil in biodiesel production then non polar diffuser will help the formation of microbubble in the system.

Conversely, for polar diffuser the oil/carboxylic acid behaves like layer spread over the surface of the diffuser. Alcohol vapours, instead of coming out in the form of smaller bubble tend to lift the "layer" of oil. This yields imbalance in flow distribution, with large amount of alcohol vapours passing through the diffuser where the pores are large and creates larger bubbles. Bubbles, significantly different from each other rise in turbulent regime and consequently coalesce to produce even larger bubbles. It decreases the surface area of the bubble, mass transfer between the reactant and also the rate of the reaction [14,20]. The overall result will be reduced mass transfer and reaction rate. Smaller bubbles also tend to rise in laminar regime ensuring less coalescence and maintaining their smaller size [16,17,21].

To examine this hypothesis, production of methyl acetate (MeAC) was investigated as an application, due to its commercial importance. It is used in resins, coating and paint, cosmetic as a solvent and as imitation fruit flavouring [7,22]. It is also used as weak polar solvent and soluble in water, with the increase in temperature its solubility increase gradually [23]. There are two methods that are commercially used for the production of MeAC, one is carbonylation and other is esterification reaction. Carbonylation process is only economically feasible where carbon mono oxide is present at site as by product [24]. So esterification reaction is widely used for the production of MeAC. In this fisher esterification reaction, the methanol (MeOH) and acetic acid (AcOH) react in the presence of the catalyst to form MeAC [25]. as shown in Eq. (1).

$$CH_3OH + CH_3COOH \rightarrow CH_3COOCH_3 + H_2O \quad (1)$$

Cost is an important factor in new developing technologies. Usually cost are defined as in capital investment of the process and in its energy requirements. Currently, the process that are used by the world for MeOH production is complicated and required high capital cost due to its complicated process design [26]. The purposed process in this study is very simple and cost effective due to its high conversion and ability to limit establishment of equilibrium. With the increase of overall conversion, the separation of final product become easy and its decreases

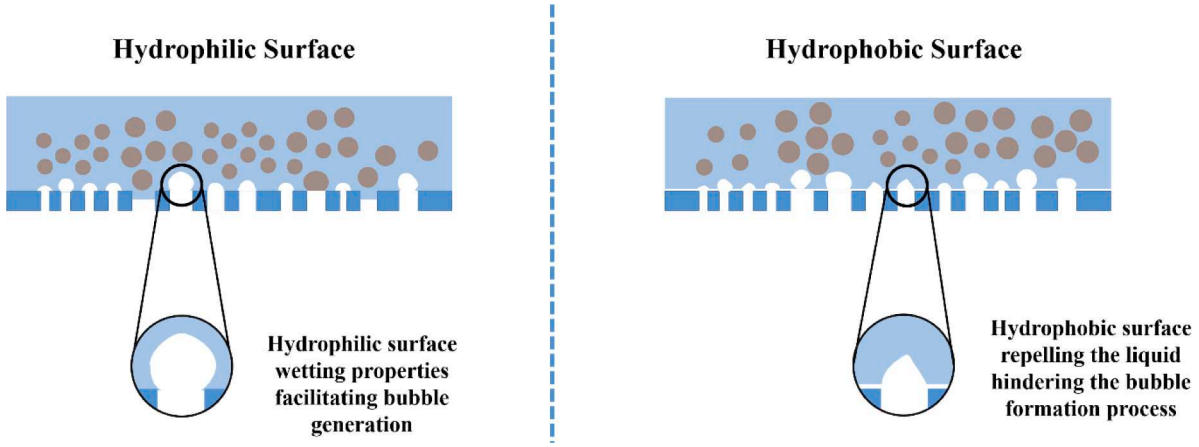

Fig. 1. The effect of the nature of the surface of diffuser on bubble generation mechanism.

the energy requirements of process that ultimately decrease the operational cost of the process.

The experimental design has been produced by Response Surface Methodology (RSM). RSM is a statistical and mathematical technique which optimize and analyse a process which is dependent on various parameters [27,28]. It generates a polynomial function that relates the response to the process variables and their interaction. The objective of this tool is to study the simultaneous and interactive effects of different parameters such as molar ratio, catalyst loading, pre-mixing time and head on the MeAC production and to optimize these process parameters. Besides RSM modelling, this study considered modelling Recurrent Neural Network technique, GRU, to correlate the response and process variables under study. Different model evaluation criterion such as R^2, MAPE, and MEDAE were employed to compare the results of RSM and GRU modelling. The detailed kinetic study for gas-liquid contraction has been studied for MeAC w.r.t microbubble process.

2. Materials and method

2.1. Reactor design

Experiments were carried out in a glass reactor fitted with a grade 1 diffuser made with borosilicate having 90 to 150 μm porosity with a total volume of 0.692 dm^3. Thermocouple (Digital Thermometer. CE) and a bourdon gauge (WIKA range 0 to 300 mbar) were used for the continuously monitoring of the temperature and pressure respectively. Silicon rubber beaker heater (Brisk Heater Corporation, USA) was used to maintain the temperature of the reactor. A round bottom flask of 500 ml was used as a MeOH vaporizer. The round bottom flask was heated using a heating mantle temperature sensor and a thermostat shown in Fig 2.

2.2. Materials and reagents

Reagent grade AcOH and MeOH was bought from DAEJUNG Chemicals, Korea. Analytical grade MeAC and phosphoric acid and acetonitrile was purchased from Sigma Aldrich. Industrial grade Para-Toluene Sulfonic Acid (PTSA) was bought from the Sentron Asia, Pakistan.

2.3. Experimental procedure

For each experiment given in Table S-II, specific amount of AcOH according to the molar ratio was premixed with PTSA in a 500 ml beaker at 70 °C and 600 rpm. Beaker was placed on a heating mantle and temperature of heating mantle was set at 70 °C. According to molar ratio, the calculated amount of MeOH was poured in a 500 ml round bottom flask as shown in Fig-2. The premixed AcOH and PTSA was added in microbubble reactor, once the MeOH started to boil at 65 °C and atmospheric pressure. The methanol vapours passed through the sintered borosilicate diffuser to produce microbubbles. The temperature of the reactor was maintained at 70 °C using the brisk beaker heater (USA) to ensure MeOH vapours do not condense in the reactor. The microbubbles rose through the AcOH present in the reactor and started the reaction on bubble surface. The vapours of the product, methyl acetate (MeAc) were condensed using a water-cooled condenser connected with reactor shown in Fig. 2.The experiments were designed and optimized using RSM for the parameters, pre-mixing time (10–80) min of Catalyst and AcOH before entering the reactor, molar ratio (1–4) of MeOH to AcOH, catalyst loading (0–4 g wt.%), and AcOH head in the reactor (0.5–2 inches) that is the height of AcOH in the reactor from the diffuser.

To investigate the kinetics of the reaction, the experiments were performed at the optimized reaction conditions; 70 ºC, 0.75 mol of AcOH, 1 mole of MeOH, and 0.5wt% (of AcOH) catalyst. First a base line of MeOH was drawn in the round bottom flask and then calculated amount of MeOH mentioned in above line was poured in the flask. The flow rate of the methanol i.e. 2 ml/*sec* was remained constant and the required amount of methanol according to the molar ratio was fed in the form of bubble of average size 800 um by prolonging the reaction time. The reaction was completed when all of the MeOH above the base line was evaporated. The reaction was completed in 20 min. First sample was taken after 5 min and then others were taken regularly at an interval of 2 min and the last one taken after 3 min of 2nd last sample. All

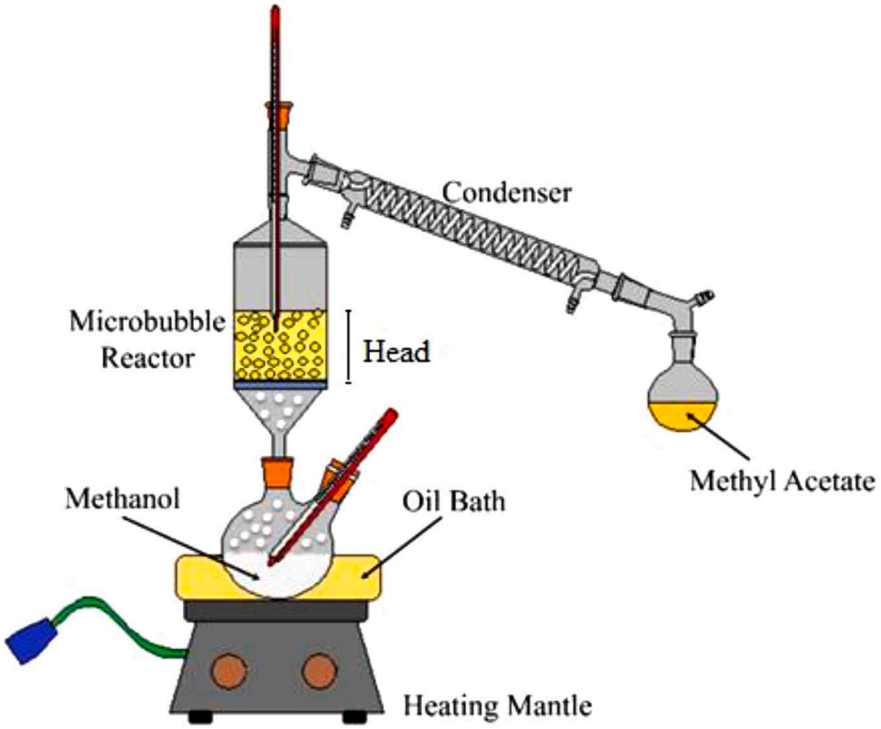

Fig. 2. Simplified microbubble process assembly.

experiment was repeated three times for standard error calculations. Following Eqs. (2) and 3 are used to calculate the molar ratio of MeOH and AcOH.

$$Volume\ for\ AcOH = \frac{Moles\ of\ AcOH * MW\ of\ AcOH}{Density\ of\ AcOH} \quad (2)$$

$$Volume\ of\ MeOH = \frac{(Moles\ of\ MeOH * n) * MW\ of\ MeOH}{Density\ of\ MeOH} \quad (3)$$

where $n = 1, 2, 3$ etc.

2.4. Analytical method

HPLC (Agilent infinity 1260) system was used to analyse the samples, the system had UV/Vis and run with chem-station software. The temperature and wavelength were set at 40 °C and 200 nm respectively in the column. Agilent zorbax C8 with particle size 5 um and 250 mm × 4.6 mm was used for analysis. 0.03 molar solution of H_3PO_4 in water and acetonitrile was used as mobile phase in ratio 88:12 v/v. 20 μL sample was injected. Linear regression was used to construct the calibration curve between concentration and observed peak area [19].

2.5. Experimental design using RSM

In the current study, Box-Bhenken Design (BBD) has been used to investigate the individual and the interactive effects of the variables molar ratio of MeOH and AcOH (A), catalyst loading (g) (B), pre-mixing time (C), and head (D) on MeAC production. The bubbling rate is fixed. However, the required amount of methanol according to the molar ratio was fed by prolonging the reaction time. Since the molar ratio at the start of the experiment cannot varied, the effect of feeding larger amount of methanol, according to molar ratio, can only be assessed by increasing the reaction time and consequently measuring the overall reaction time. The upper and lower range of the parameters were given to the software - A (1–4), B (0–4 g wt.%), C (10–80 min), and D (0.5–2 inches). A total of 29 experiments were designed as given in supplementary data as Table-S2. The experiments were performed accordingly and their response were measured.

2.6. Statistical analysis (ANOVA: Analysis of variance)

Fit summary as shown in Table 1 suggests that the most adequate model for fitting the experimental data is quadratic model. The accuracy of this model was elaborated by Analysis of Variance (ANOVA). It gives main and interactive effects of the variables, and the error terms included in the model. The significance of the parameters is verified by *p*-value and F-value in the model [29]. The parameters having larger F value and *p*-value <0.05 are considered to be significant. In this case A, B, AB, AD, B^2 are significant model terms given in supplementary data as Table SIII. The effects of all the parameters have been discussed in detail in Section 4.2 to onward. The accuracy of the quadratic model was also accessed by correlation coefficient (R^2), predicted R^2, and adjusted R^2 given in Table 2. R^2 closer to one shows that the actual data closely fits the data predicted by RSM model [30]. The quadratic model in the present study has 0.971 R^2 which shows accurate fitting of the model.

Table 1
Fit summary of the model.

Source	Sequential *p*-value	Lack of Fit *p*-value	Adjusted R^2	Predicted R^2	
Linear	< 0.0001	< 0.0001	0.5902	0.4550	
2FI	0.0159	< 0.0001	0.7518	0.4947	
Quadratic	< 0.0001	< 0.0001	0.9430	0.8361	Suggested
Cubic	0.0200	0.0003	0.9855	0.5612	Aliased

Table 2
ANOVA for Response Surface Quadratic Model.

Standard terms	Value	Standard terms	Value
Std. Dev.	0.0329	**R^2**	0.9715
Mean	0.4787	**Adjusted R^2**	0.9430
C.V.%	6.87	**Predicted R^2**	0.8361
		Adeq. Precision	21.3866

Adjusted R^2 gives better accessibility of the model fitting than R^2 since it also includes the effect of insignificant terms present in the model [31]. Here the Adjusted R^2 is 0.943. The value of adequate precision which is greater than i.e., 21.83 also supports the fitness of the model as per design expert software [32]. The model also gives *p*-value for the lack of fit less than 0.0001 which shows that linear regression model does not fit the data well and quadratic model is the true representation of the data.

2.7. Artificial intelligence model

For the prediction of response, conversion%, artificial intelligence modelling was also incorporated using 29 samples of the data. The performance of artificial intelligence models is contingent on both the quantity and quality of data, as well as the choice of modelling algorithm. Certain algorithms are more appropriate for modelling with limited data. Among the algorithms that are suitable for this purpose are support vector machine, Gaussian process regression, random forest, gradient boosting decision tree, XGBoost, symbolic regression, and artificial neural network [33].

For this study Recurrent Neural Network (RNN) using Gated recurrent unit (GRU) was opted for modelling purpose that requires suitable value of hyperparameters such as number of hidden units, gradient threshold, initial learning rate, learn rate drop factor, and learn rate drop period. The GRU model architecture was designed by changing hypermeters. Different model evaluation criteria such as R^2, Mean Absolute Percentage Error (MAPE), and Median Absolute Error (MEDAE) were employed to select the best parameter for the model architecture given in Supplementary data as Table S-IV.

RSM model has reported 0.9715 R^2 that shows good fitting efficiency Fig. 3. However, GRU has shown even more superior efficiency and reported 0.9981 R^2. Besides, other performance evaluation criteria have reported outperforming prediction capability of GRU compared to RSM model Table 3. Table 3 confirms the superiority of the GRU model as its predicted values are in good agreement with actual values Fig. 4. From Fig. 3(a) deviating RSM model prediction values from actual values are clearly visible causing lower R^2, and larger MAPE and MEDAE compared to GRU model Fig. 4(a). The MAPE for RSM model is 3.908 that is approximately double compared to GRU model 1.7615. Furthermore, MEDAE for GRU model 0.0027 confirms its superiority over RSM model 0.0152.

Scatter figure comparison between actual and predicted values of RSM (Fig. 3 (b)) and GRU (Fig. 4 (b)) also confirms the superior prediction performance of the GRU model. A 45-degree line has been added to assist the interpretation of the scatter figures. Predicted points closer to the 45-degree line contribute towards higher R^2, and lower MAPE and MEDAE. It can be analysed that RSM predicted values deviates more from 45-degree line compared to GRU predicted values. This also confirms the superior prediction capability of the GRU model compared to RSM model.

3. Reactions kinetics

In this work esterification is carried out in a bubble reactor. The rate of the reaction in this case depend upon the mass transfer and the reaction kinetics of the chemical reaction. The results are highly dependent on the mechanism, and is referred in the section of results and analysis, it is very important to develop a sturdy understanding of the

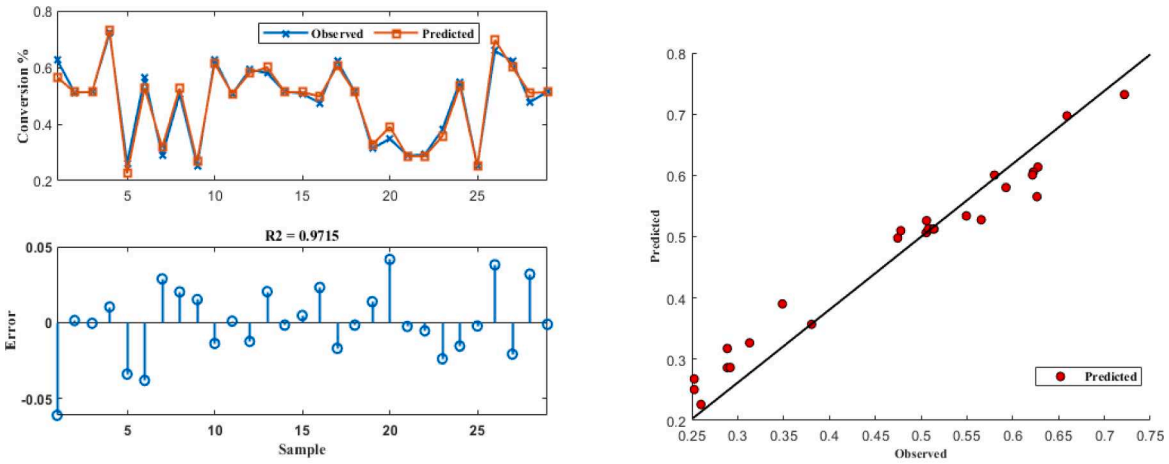

Fig. 3. RSM model performance **(a)** RSM model prediction **(b)** RSM Model prediction scatter plot.

Table 3
Performance criteria comparison (RSM vs GRU).

Criteria	Conversion% prediction performance	
	RSM Model	GRU Model
$\mathbf{R^2}$	0.9715	0.9981
MAPE	3.908	1.7615
MEDAE	0.0152	0.0027

mechanism of the reaction. The reaction mechanism is given below from Eqs. (4) to (9). In the beginning the catalyst (PTSA) is ionized and losses its proton as shown in first Eq. (4). The proton from PTSA attacks on the AcOH and protonate it as shown in Eq. (5). In Eq. (6), a lone pair of electrons from oxygen in the alcohol molecule attack on the AcOH, the electrophile, and make nucleophilic substitution. This is the rate limiting step. In Eq. (7) and Eq. (8), the charge transfers from oxygen atom to the central carbon atom followed by the elimination of proton to form MeAC. In the last step, the eliminated proton is re-attach with the PTSA ion to regenerate it [34].

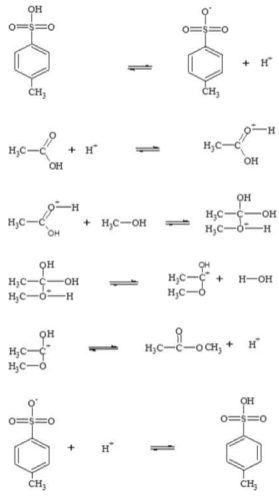

(4)

(5)

(6)

(7)

(8)

(9)

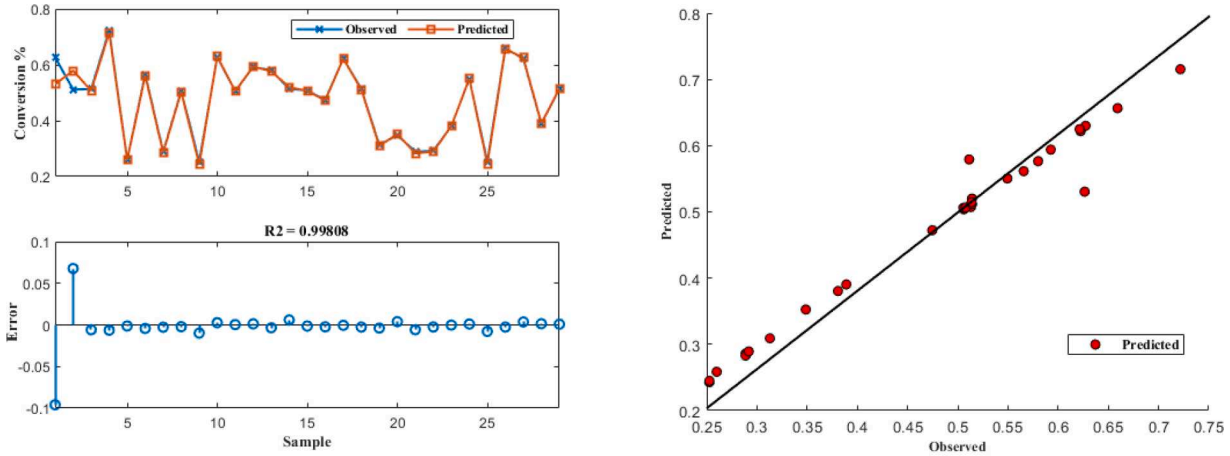

Fig. 4. GRU model performance **(a)** GRU model prediction **(b)** GRU Model prediction scatter plot.

Conventionally, the reaction is carried out in the bulk. The literature has reported both first and second order for the esterification depending upon the reactor configuration [35]. For the current study, where the reaction is carried out between vapour-liquid phases. It is very important to investigate the kinetics of the reaction and analyse if the reaction occurs on the skin of the bubble or not. The control volume to assess the kinetics of the process is shown in Fig 5. There are many several models are used along with two film theory. These theories or models state that the liquid at interface continuously removed or washed by fresh fluid from the main body of the liquid and that's how mass transfer occur. These models are also different from a physical standpoint and give essential identical prediction of steady state behaviour. Due to these reasons, two film theory as adopted by Levenspil method was used to analyse the kinetics [23]. It must also be noted that under the current reaction conditions, only gas diffuse in liquid and the concentration of liquid (Acetic acid C_b) does not drop in large quantity with in the film.

To determine whether the reaction is kinetics controlled or diffusion controlled, Hatta number (M_H) was calculated If $M_H < 1$, it shows the reaction occurs in the bulk section and diffusion of reactants in bulk will be the controlling factor. If $M_H > 1$ then it shows, the reaction takes place on the surface of the bubble and controlling factor will be the surface area [36,37]. The equation of M_H is shown below.

$$M_H = \frac{\sqrt{(D_{ab})kC_b}}{k_{bl}} \tag{10}$$

where D_{ab}, k and K_{bl} are the diffusion coefficient of MeOH and AcOH, rate constant and liquid film coefficient respectively. C_b is the concentration of acetic acid and relate in liquid phase. D_{ab} was calculated using Eqs. (11) and (12) at 25 °C and at 70 °C respectively [38];

$$(D_{ab})_{T=25oC} = 6.02 * 10^{-5}\left(\frac{V_b^{0.36}}{\mu_b^{0.61}V_a^{0.64}}\right) \tag{11}$$

$$(D_{ab})_T = 4.996 * 10^3 (D_{ab})_{T=25oC}\exp\left(\frac{-2539}{T}\right) \tag{12}$$

K_{bl} was calculated for bubble less than 2 mm in diameter by the following Eq. (13)

$$k_{bl} = 0.31\left(\frac{(D_{ab})_T\rho_b g}{\mu_b}\right)^{1/3} \tag{13}$$

M_H was found to be greater than 1 which confirm that the reaction was kinetically dominating and occurred on the surface of the bubble. Enhancement factor (E) was used to calculate the order of the reaction using Eq. (14). If $E_i > 5$ M_H then we have pseudo first order reaction by the gas/Liquid interface in which case $E \cong M_H$ more precisely it follow the following equation.

$$E = M_H\left(1 - \frac{M_H - 1}{2E_i}\right) \tag{14}$$

3.1. Infinite enhancement factor (E_i) was calculated by Eq. (15) [36]

$$E_i = 1 + (D_{ab})_T\left(\frac{C_B H_A}{bP_A}\right) \tag{15}$$

where, P_A and C_B are the partial pressure and concentration of MeOH and H_A is Henry`s constant. The reaction was found to follow pseudo-first order kinetics as the value of Enhancement factor (E) was approximately equal to the Hatta number M_H. By using the values of E, M_H, and E_i from the rate of reaction for the bubble mediated esterification reaction was measured;

$$-r_A = \frac{P_A}{\frac{1}{k_{Ag}\sigma} + \frac{H_A}{\sqrt[a]{(D_{ab})_T kC_B}}} \tag{16}$$

where, P_A and K_{AG} are the overall pressure in (bar) and mass transfer in gas film coefficient respectively. The value of rate constant (k) is 7.266 Kmol/s m^3 and liquid film coefficient (K_{bl}) is 2.82×10^{-4} m/s was calculated using the concentration and time graph as see in Fig. 1 [39]. The overall rate of the esterification reaction is given below in Eq. (14), and units of r_A were Kmol/s m^3. For comparison, various rate expression have been in listed in supplementary data as Table S8.

$$-r_A = \left(4.247 \times 10^{-7}\right)(P_A \times 101,325)\left(\sqrt{C_B}\right) \tag{17}$$

4. Results and discussions

4.1. Comparison of gas-liquid system with conventional system

The major difference between the conventional liquid-liquid technique and the microbubble process that is discussed in this study must be elaborated. In conventional liquid-liquid process, the required amount of catalyst and reactants are mixed together. The reaction takes place in the bulk system. The reaction depends upon the protonation of the AcOH as it makes AcOH labile for subsequent MeOH attack. Since, the reactants are liquid and miscible with each other and T and P is constant, the only constraint effecting the equilibrium is the reaction kinetics. As discussed above, the acid catalysis follows reaction in a series mechanism. Additionally, development of an early equilibrium because of production of water, the reaction has low reaction rate. The maximum conversion achieved in conventional system/control is 20% in 30 min.

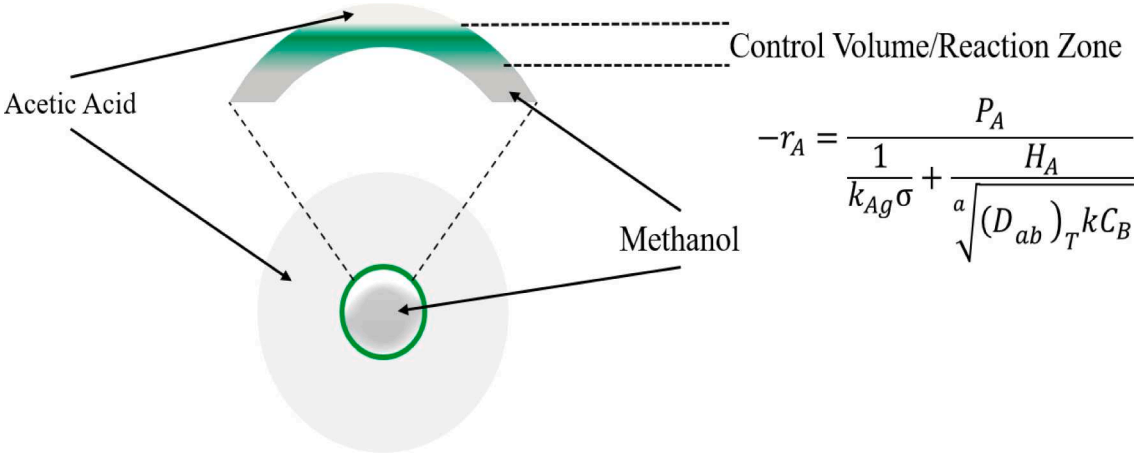

Fig. 5. Interfacial interaction between MeOH (vapour) bubble and Acetic acid.

However, in microbubble mediated process the reaction takes place on the surface of the bubble. In the current study, the MeOH is fed in the reactor in the form of microbubbles. As discussed above, the bubbles have high surface area to volume ratio due to its small size enhancing the mass and heat transfer [14]. The microbubble of MeOH has low buoyancy forces causing the microbubble to rise slowly. As it rises, it keeps on reacting with the "fresh" and protonated AcOH. The product is formed on the skin of the bubbles, diffuses towards the centre of the bubble and the conversion of the MeAC increases as shown in Fig. 6. Eventually the microbubble bursts at the surface. The unreacted alcohol and products of the reaction leave the system which prevent the establishment of equilibrium in the system.

As seen in the Fig. 7, approximately 70% conversion was achieved in first 10 min and a total conversion of 91% is achieved in 20 min with a standard error of **3%**. This high conversion and rate of reaction can be attributed to several factors.

One of the important factors is the protonation of the AcOH before the reaction by premixing with catalyst. AcOH is not the rate limiting step, however, as seen previously it does effect the overall conversion and rate of reaction [14,19,40]. As discussed above, it makes the AcOH labile for an instant attack from MeOH. Another important factor is the internal mixing by the microbubbles of the MeOH. Due to the internal mixing, the product formed at the skin of the bubbels fluxes in the bubble while the alcohol moves out at the interface. As the microbubble rise, it always have fresh AcOH and MeOH all the time increasing the conversion and rate of the reaction [41]. It must also be noted, that the MeOH is simultaneously removed from the system because the reaction is carried out at a higher temperature than its boiling point 64.7 °C. Another interesting point is that the temperature of acetic acid is 70 °C and vapour of methanol is coming at its boiling point that is 65 °C. There is a temperature gap between liquid and vapour due to which heat is transferring from liquid to vapour through interface and also the methyl acetate reaction is slightly exothermic reaction with −9kj/km heat of reaction. Third liquid acetic acid have high heat capacity as compare to the methanol vapour due to their density difference. Due to all these factors it can be assumed that the temperature of the interface or surface is higher as compare to the system. Consequently, a very high conversion and high reaction rate has been achieved as compared to previously reported results as shown in Table 4.

4.2. Diagnostic plots

The Perturbation plot given in supplementary data in Fig S-I, shows the relation between the different variable and their responses (conversion). Deviation of the variable from the reference point highlights the change in conversion. Fig. 8 demonstrated, the catalyst loading (B) is the most influential factor as compare to the other three. At zero catalyst loading, there is significantly low conversion. Larger catalyst loading means that large amount of AcOH will be protonated and, consequently, yield high conversion. So a steep rise is observed in seen in Fig S-I. Molar Ratio (A) is the second influential factor and have inverse relation with conversion. With the increase in the molar ratio, the amount of the unreacted alcohol is also increased which can accumulate in the reactor and mimic a liquid-liquid equilibrium similar to what is observed in in conventional system and reduces the conversion.

Premixing time (C) has almost a straight line in Fig S-I. Apparently, it seems that it does not affect conversion significantly as compared to catalyst loading and molar ratio. However, the effect of Premixing can be easily misinterpreted. As discussed above, premixing the catalyst with the AcOH yields made carbonium ion. The graph also indicate that the premixing does not affect the conversion significantly, it emphasizes that the maximum ionization of AcOH has already occurred before the 10 min. This is shown by a significantly low conversion of 24.8% in the control experiment carried out without premixing. The result of control experiment is shown that there is a difference in conversion without premixing. The acid catalytic esterification reaction follow reaction in series where the acetic acid is first protonated and then follow the attack of methyl radical. So having acetic acid in protonated state assists the reaction instantaneously [19,40,46].

Parameter D, the head of AcOH in the reactor, has significantly low effect on the conversion. By increasing the head, the conversion did not increase significantly. As demonstrated in the kinetics, the reaction is kinetics controlled and is carried out on the skin of the bubble. The product fluxes in the centre of the bubble. Microbubbles are small and achieve mass transfer equilibrium very quickly and attains equilibrium [15,47]. This happens over a very small scale of height and the reaction

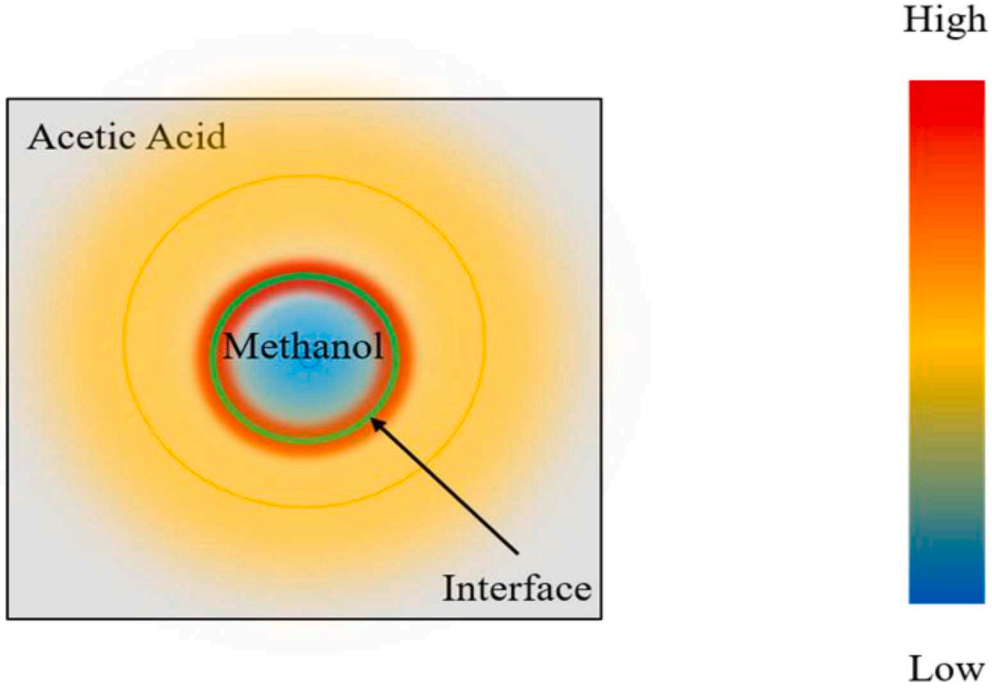

Fig. 6. Reaction of rising MeOH bubble with protonated acetic acid.

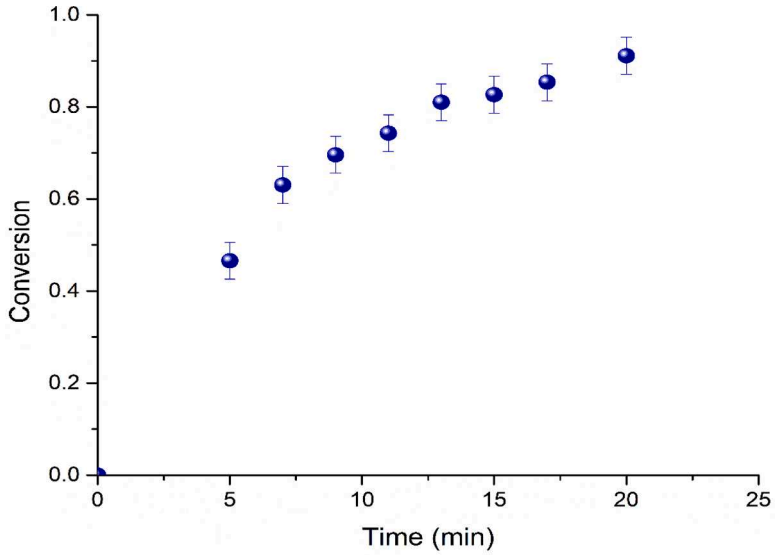

Fig. 7. Effect of time on the methyl acetate conversion.

Table 4
Comparison of conversion with previous studies.

Systems	Conversion (%)	Time (min)	Temperature (°C)	References
Simple reactive batch distillation	49.41	102	37	[42]
Pervaporation by cross-linked PVA/silica nanocomposite membranes	94	300	70	[43]
Reactive extraction	70	360	28	[44]
Using activated TiO_2 as catalyst Under UV light Radiation	79	240	30	[45]
Microbubble process	**91**	**20**	**70**	**This study**

does not proceed further. This does not mean the head of the AcOH is insignificant-however, it emphasizes the fact that tall bubble columns might not be needed for scaling up the reactor. Since, the conversion has already been achieved approximately at a head of 0.5 inch, a thin film reactor may provide equally good results.

4.3. Plot for the catalyst loading and molar ratio

The combined effect of the catalyst loading and the molar ratio on the conversion of the reaction has been shown in the Fig. 8. Without catalyst and minimum molar ratio, the conversion was significantly low. Highest conversion was achieved at the maximum catalyst loading and minimum molar ratio. Conversion was found to increase significantly with the increase in catalyst loading as it increases the protonation of the AcOH. It could also be noticed, that at minimum catalyst loading, no significant change was observed by changing the molar ratio from minimum to maximum. At minimum catalyst loading and the maximum molar ratio the conversion was comparatively low than the conversion

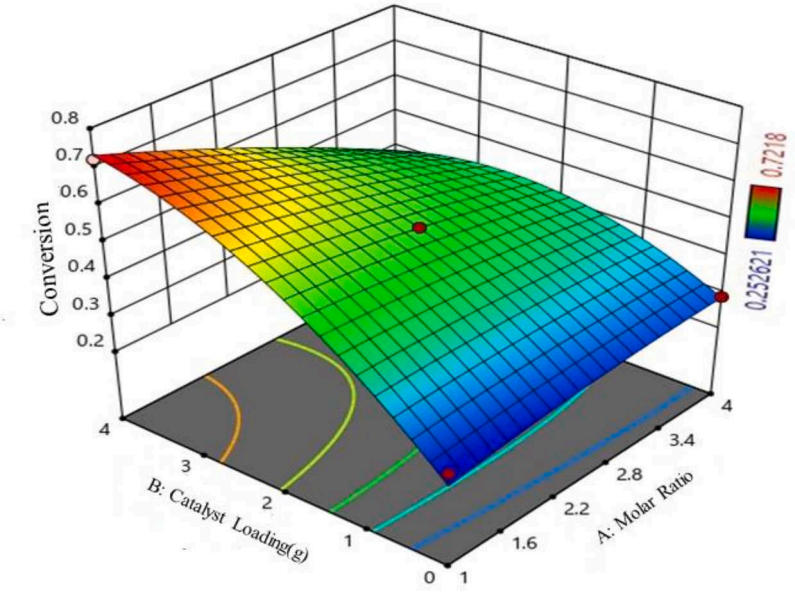

Fig. 8. Simultaneous effect of catalyst loading and molar ratio on the conversion.

achieved using maximum catalyst loading and minimum molar ratio. By increasing the molar ratio, the amount of the unreacted alcohol increased due to the accumulation of alcohol in the reactor. The accumulated alcohol and the unreacted AcOH can mimic a liquid-liquid equilibrium similar to what is created in conventional system reducing the conversion after molar ratio greater than 1:1

4.4. Plot for head and catalyst loading

The Fig. 9 shows the interactive effect of head of AcOH and catalyst loading simultaneously on the conversion of the reaction. At minimum head and without catalyst the conversion was low. Without addition of catalyst, conversion was not found to increase significantly by increasing the head gradually. By increasing the Head, the height of the AcOH increases in the reactor. As discussed above, due to higher interfacial area the mass transfer by microbubbles is fast. After rising through a head of AcOH 0.5 inch the reaction proceeding on the interface stops. At the maximum catalyst loading and minimum head the conversion was maximum because of the maximum protonation of acid. A sharp decrease in conversion is observed as catalyst loading is reduced. At maximum catalyst and maximum head, the conversion was same and no significant change was occurred.

4.5. Plot for premixing time and catalyst loading

The Fig. 10 shows the effect of premixing and catalyst loading on the conversion of the reaction. At zero catalyst loading, there is negligible protonation, so premixing the catalyst with AcOH had a very little effect on the conversion of the reaction. At minimum premixing time when catalyst loading is gradually increased, a sharp increase in the conversion is observed. It is counter-intuitive to note that at maximum amount catalyst loading and maximum premixing time the conversion of the reaction has decreased. PTSA was premixed with AcOH 70 °C. PTSA was found to decompose when premixed for longer period of time. It was also evident from the colour change of the mixture from colourless to brownish colour. PTSA decomposes and releases SO_2 which when dissolved produced brown colour. With less amount of catalyst, the protonation is minimized and lower value of conversion is achieved.

4.6. Plot for of head and molar ratio

The Fig. 11 shows an interactive plot between, the conversion of the reaction, the head of AcOH and molar ratio of the reactant. At minimum molar ratio and head the conversion of the reaction is maximum. At lower head, the change in the molar ratio had the inverse relation with conversion. By increasing the molar ratio, the amount of unreacted alcohol in the system increased and have a bad impact on the conversion as shown in Fig S-I. At lower molar ratio, the change in head had the inverse relation with the conversion. By increasing the head the amount of AcOH in the reactor increased and since the molar ratio was constant so gradually the amount of alcohol also increased. As discussed above in Fig. 8 after the 0.5 inch head no reaction occur so the amount of alcohol that was increased to maintain the molar ratio causing the liquid-liquid equilibrium in the system that decreased the overall conversion.

4.7. Plot for head and premixing time

The Fig. 12 shows the combined effect of the head and premixing time on the conversion of the reaction. At low premixing time, the head of AcOH had a very negligible effect on the conversion. Increasing head also increases the required amount of AcOH. There was a negligible effect of increasing the amount of AcOH on the conversion after a certain height due to the decrease in mass transfer. At low head premixing had no effect on the conversion due to the maximum protonation of the AcOH has already taken place before the 10 min of premixing time. At maximum head and premixing time the conversion decreased. As discussed above, with increase in premixing time PTSA starts to decompose.

4.8. Plot for molar ratio and premixing time

The combined effect of the premixing time and the molar ratio of the reaction on the conversion has been shown in the Fig. 13. At low molar ratio when premixing time was increased, a slight increase in the conversion was observed because of the protonation of AcOH. When molar ratio increased at low premixing time the negligible increase was occurred in the conversion. When both the molar ratio and premixing

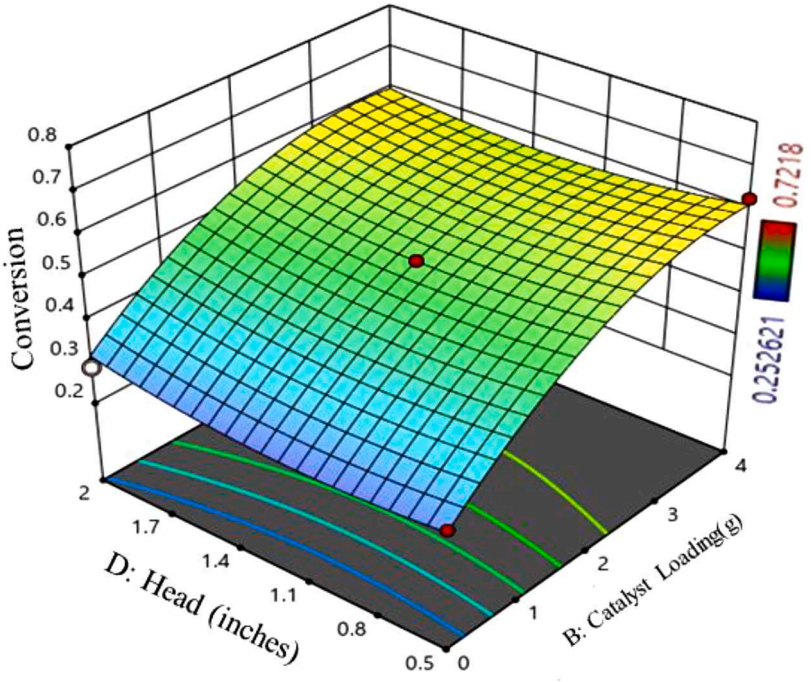

Fig. 9. Simultaneous effect of Head and catalyst loading on the conversion.

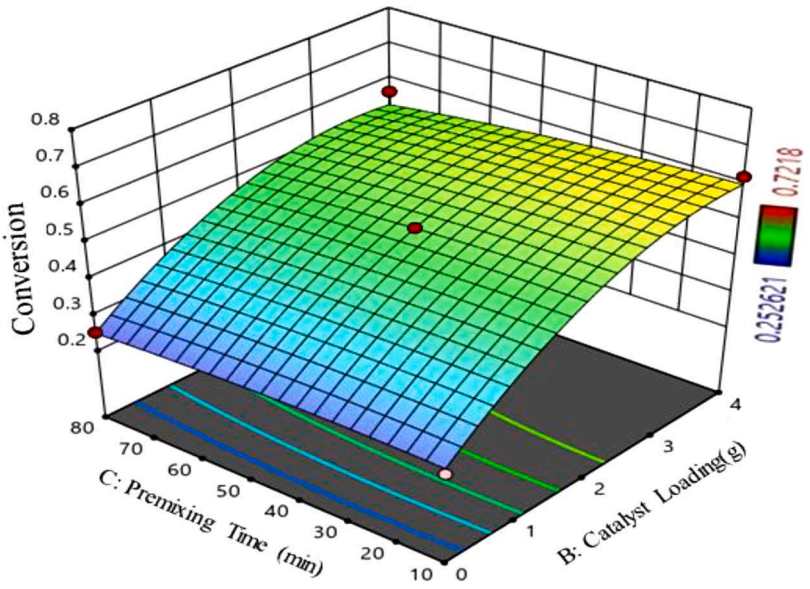

Fig. 10. Simultaneous effect of premixing time and catalyst loading on the conversion.

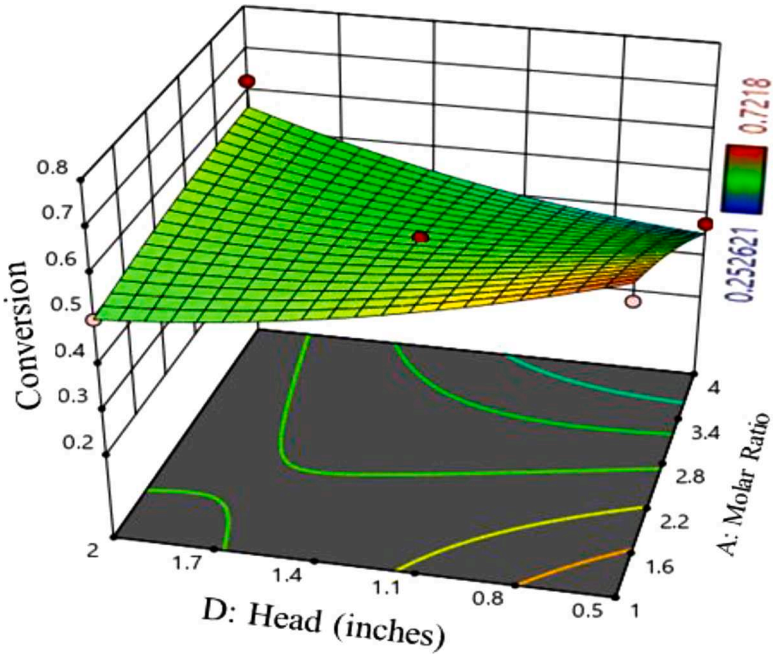

Fig. 11. Simultaneous effect of Head and Molar Ratio on the conversion.

time increased simultaneously the conversion of the reaction was found to decrease. Again, at maximum molar ratio the amount of unreacted alcohol increased by accumulation in the reactor. Conversion was found to decrease with the increase in premixing time because of the decomposition of PTSA.

5. Conclusion

The conventional production method for the esterification reaction is very energy and time-intensive due to the mass transfer and equilibrium limitations. In the study, the MeAC was produced as an application of vapour-liquid system in which the MeOH bubbles are fed in the liquid AcOH. As the microbubbles have a high volume to surface area ratio, which increased the reaction rate and moves the equilibrium in the forward direction. Kinetics of the reaction show that reaction is pseudo first order and reaction is occurring on the surface of the bubble of the methanol. The final rate equation show that reaction is mainly depend upon the concentration or pressure of the methanol. When reaction occur on the surface of the bubble, product started to accumulate around the bubble and when it burst on the surface, product and unreacted methanol left the system. This process pulls the reaction toward the completion and prevent the establishment of the equilibrium. In the current study, the kinetics of reaction shows that the 70% conversion in the first 10 min and 91% conversion in 20 min that is significantly higher than previously reported studies. Several parameters have been investigated to optimize the MeAC production using RSM. The catalyst loading and the molar ratio of reactants were found to be significant parameters. As the catalyst loading increases, the conversion tends to increases and achieved 72.5% at the minimum molar ratio. Approximately 60% conversion was achieved for both minimum and maximum

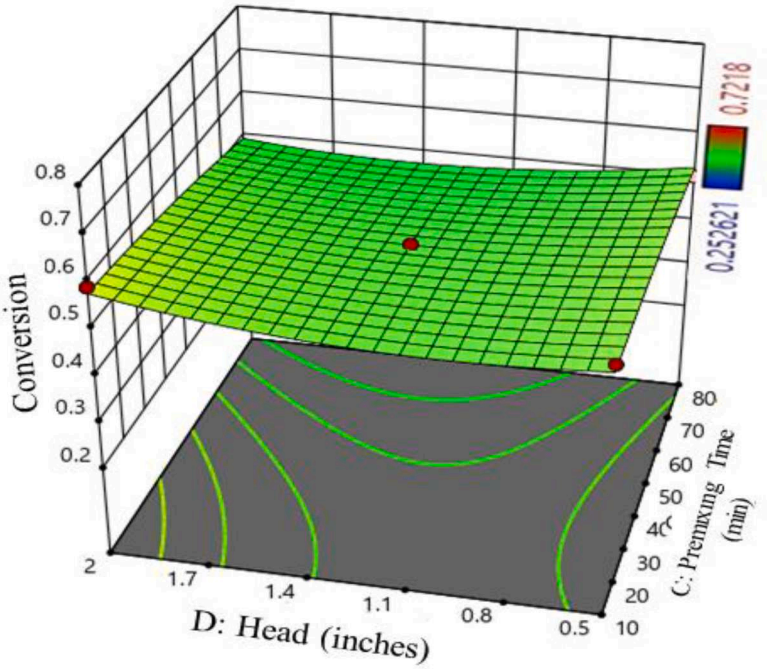

Fig. 12. Simultaneous effect of Head and Premixing time on the conversion.

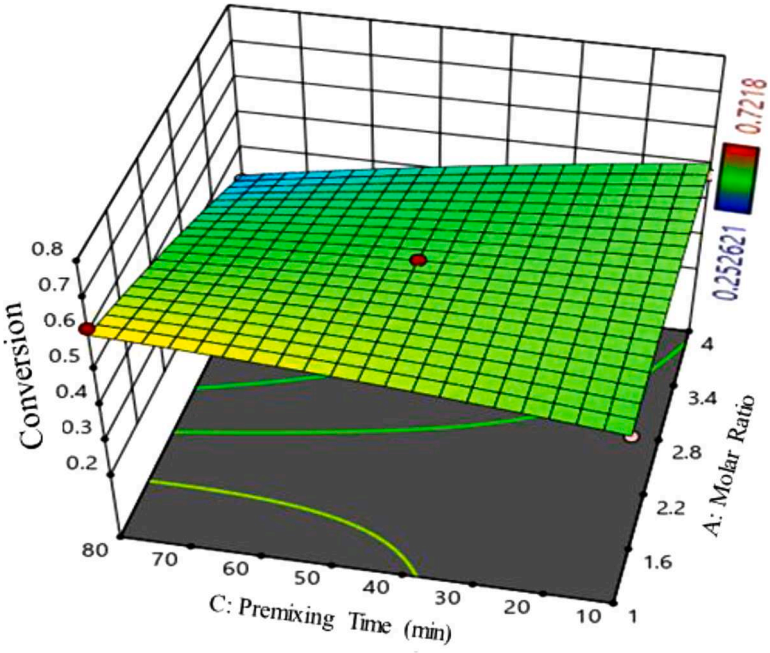

Fig. 13. simultaneous effect of molar ratio and pre-mixing time on the conversion.

head change. For minimum and maximum premixing time conversion varied from 50 to 60% at maximum catalyst loading. 25% conversion was achieved at low catalyst loading and maximum premixing time. The results demonstrate the current gas-liquid reaction system has a high potential for several applications of esterification reactions at industrial scale which are limited by poor mass transfer, low conversion and a low reaction rate. GRU modelling was also experimented by employing required hyperparameters bound values to opt the best performing model architecture. The experimentation provided number of hidden units 141, gradient threshold 0.01, initial learning rate 0.0099, learn rate drop factor, 0.1, learn rate drop period 131, and training epoch 150 as optimized hyperparameters. Using optimized hyperparameters GRU model was also developed to predict the response and compare the results with the RSM model The performance criteria values of R^2, MAPE and MEDAE were 0.9981, 1.76157 and 0.0027 for GRU and 0.9715, 3.908 and 0.0152 for RSM respectively. Compared to RSM, GRU depicted enhanced performance with higher R^2 value, approximately half MAPE value and approximately five times lower MEDAE value. GRU model could be used for robustly predicting the conversion% of the process.

CRediT authorship contribution statement

Talha Istkhar: Data curation, Writing – original draft. **Ainy Hafeez:** Methodology. **Fahad Javed:** Formal analysis. **Tahir Fazal:** Formal analysis. **Faisal Ahmad:** Software. **Arif Hussain:** Software. **William B. J. Zimmerman:** Funding acquisition. **Fahad Rehman:** Conceptualization, Supervision, Funding acquisition.

Declaration of Competing Interest

The authors declare that they have no known competing financial interests or personal relationships that could have appeared to influence the work reported in this paper.

Data availability

Data will be made available on request.

Acknowledgement

Authors want to acknowledge the Higher Education Commission Pakistan (HEC) for their funding under the National Research Program for Universities (NRPU) Project Number 20-7924/19. Fahad Rehman and William Zimmerman would like to acknowledge the research grant EP/S031421/1 from Engineering and Physical Sciences Research Council, UK.

Supplementary materials

Supplementary material associated with this article can be found, in the online version, at doi:10.1016/j.cep.2023.109435.

References

[1] J. Otera, J. Nishikido, Esterification: methods, reactions, and Applications, John Wiley & Sons, 2009.
[2] Y. Liu, E. Lotero, J.G. Goodwin Jr, Effect of water on sulfuric acid catalyzed esterification, J. Mol. Catal. A Chem. 245 (2006) 132–140.
[3] B. Zhou, Y. Fang, H. Gu, S. Zhang, B. Huang, K. Zhang, Ionic liquid mediated esterification of alcohol with acetic acid, Front. Chem. Eng. China 3 (2009) 211–214.
[4] Y.-H. Chung, T.-H. Peng, H.-Y. Lee, C.-L. Chen, I.-L. Chien, Design and control of reactive distillation system for esterification of levulinic acid and n-butanol, Ind. Eng. Chem. Res. 54 (2015) 3341–3354.
[5] J. Marchetti, A. Errazu, Technoeconomic study of supercritical biodiesel production plant, Energy Convers. Manage. 49 (2008) 2160–2164.
[6] B. Bessling, J.M. Löning, A. Ohligschläger, G. Schembecker, K. Sundmacher, Investigations on the synthesis of methyl acetate in a heterogeneous reactive distillation process, Chem. Eng. Technol. Ind. Chem.-Plant Equip.-Process Eng.-Biotechnol. 21 (1998) 393–400.
[7] R.S. Huss, F. Chen, M.F. Malone, M.F. Doherty, Reactive distillation for methyl acetate production, Comput. Chem. Eng. 27 (2003) 1855–1866.
[8] M.A. Santaella, A. Orjuela, P.C. Narváez, Comparison of different reactive distillation schemes for ethyl acetate production using sustainability indicators, Chem. Eng. Process. Process Intensification 96 (2015) 1–13.
[9] R. Ran, J. Li, G. Wang, Z. Li, C. Li, Esterification of methacrylic acid with methanol: process optimization, kinetic modeling, and reactive distillation, Ind. Eng. Chem. Res. 58 (2019) 2135–2145.
[10] P. Seferlis, J. Grievink, Optimal design and sensitivity analysis of reactive distillation units using collocation models, Ind. Eng. Chem. Res. 40 (2001) 1673–1685.
[11] Y.T. Tang, H.-P. Huang, I.-L. Chien, Design of a complete ethyl acetate reactive distillation system, J. Chem. Engi. Jpn. 36 (2003) 1352–1363.
[12] S. Hernandez, R. Sandoval-Vergara, F.O. Barroso-Muñoz, R. Murrieta-Dueñas, H. Hernández-Escoto, J.G. Segovia-Hernández, V. Rico-Ramirez, Reactive dividing wall distillation columns: simulation and implementation in a pilot plant, Chem. Eng. Process. Process Intensification 48 (2009) 250–258.
[13] J. Keogh, M.S. Tiwari, H. Manyar, Esterification of glycerol with acetic acid using nitrogen-based Brønsted-acidic ionic liquids, Ind. Eng. Chem. Res. 58 (2019) 17235–17243.
[14] N. Ahmad, F. Javed, J.A. Awan, S. Ali, T. Fazal, A. Hafeez, R. Aslam, N. Rashid, M. S.U. Rehman, W.B. Zimmerman, Biodiesel production intensification through microbubble mediated esterification, Fuel 253 (2019) 25–31.
[15] W.B. Zimmerman, V. Tesar, S. Butler, H.C. Bandulasena, Microbubble generation, Recent Patents Eng. 2 (2008) 1–8.
[16] F. Rehman, Y. Liu, W.B. Zimmerman, The role of chemical kinetics in using O3 generation as proxy for hydrogen production from water vapour plasmolysis, Int. J. Hydrogen Energy 41 (2016) 6180–6192.
[17] F. Javed, Z. Shamair, S. Ali, N. Ahmad, A. Hafeez, T. Fazal, M.S.U. Rehman, W. B. Zimmerman, F. Rehman, Pushing and pulling" the equilibrium through bubble mediated reactive separation for ethyl acetate production, React. Chem. Eng. (2019).
[18] W.B. Zimmerman, R. Kokoo, Esterification for biodiesel production with a phantom catalyst: bubble mediated reactive distillation, Appl. Energy 221 (2018) 28–40.
[19] F. Javed, Z. Shamair, S. Ali, N. Ahmad, A. Hafeez, T. Fazal, M.S.U. Rehman, W. B. Zimmerman, F. Rehman, Pushing and pulling" the equilibrium through bubble mediated reactive separation for ethyl acetate production, React. Chem. Eng. 4 (2019) 705–714.
[20] F. Rehman, W.S. Abdul Majeed, W.B. Zimmerman, Hydrogen production from water vapor plasmolysis using DBD-Corona hybrid reactor, Energy Fuels 27 (2013) 2748–2761.
[21] F. Rehman, G.J. Medley, H. Bandulasena, W.B. Zimmerman, Fluidic oscillator-mediated microbubble generation to provide cost effective mass transfer and mixing efficiency to the wastewater treatment plants, Environ. Res. 137 (2015) 32–39.
[22] K. Sandesh, P. JagadeeshBabu, S. Math, M. Saidutta, Reactive distillation using an ion-exchange catalyst: experimental and simulation studies for the production of methyl acetate, Ind. Eng. Chem. Res. 52 (2013) 6984–6990.
[23] O. Levenspiel, Chemical reaction engineering, Ind. Eng. Chem. Res. 38 (1999) 4140–4143.
[24] R.B. Diemer, W.L. Luyben, Design and control of a methyl acetate process using carbonylation of dimethyl ether, Ind. Eng. Chem. Res. 49 (2010) 12224–12241.
[25] M.A. Al-Arfaj, W.L. Luyben, Comparative control study of ideal and methyl acetate reactive distillation, Chem. Eng. Sci. 57 (2002) 5039–5050.
[26] D. An, W. Cai, M. Xia, X. Zhang, F. Wang, Design and control of reactive dividing-wall column for the production of methyl acetate, Chem. Eng. Process. Process Intensification 92 (2015) 45–60.
[27] A.I. Khuri, S. Mukhopadhyay, Response surface methodology, Wiley Interdiscip. Rev. Comput. Stat. 2 (2010) 128–149.
[28] S. Yang, X. Yu, Y. Zhou, LSTM and GRU neural network performance comparison study: taking yelp review dataset as an example, in: 2020 International Workshop on Electronic Communication and Artificial Intelligence (IWECAI), 2020, pp. 98–101.
[29] S.K. Behera, H. Meena, S. Chakraborty, B. Meikap, Application of response surface methodology (RSM) for optimization of leaching parameters for ash reduction from low-grade coal, Int. J. Min. Sci. Technol. 28 (2018) 621–629.
[30] R.F. Gunst, Response Surface methodology: Process and Product Optimization Using Designed Experiments, Taylor & Francis, 1996.
[31] A. Hafeez, S.M.A. Kazmi, M. Sulaiman, C.H. Ali, N. Feroze, Optimization of zinc ions removal by modified phoenix Dactylifera L. seeds using response surface methodology, J. Chem. Soc. Pakistan 41 (2019), 78-78.
[32] H. Zhang, H. Li, H. Pan, A. Wang, S. Souzanchi, C.C. Xu, S. Yang, Magnetically recyclable acidic polymeric ionic liquids decorated with hydrophobic regulators as highly efficient and stable catalysts for biodiesel production, Appl. Energy 223 (2018) 416–429.
[33] P. Xu, X. Ji, M. Li, W. Lu, Small data machine learning in materials science, npj Comput. Mater. 9 (2023) 42.
[34] A. Rolfe, C. Hinshelwood, The kinetics of esterification. The reaction between acetic acid and methyl alcohol, Trans. Faraday Soc. 30 (1934) 935–944.
[35] H.A. Al-Jendeel, M.H. Al-Hassani, N.S.A. Zeki, Kinetic study of esterification reaction, Al-Khwarizmi Eng. J. 6 (2010) 33–42.
[36] T.O. Salmi, J.-P. Mikkola, J.P. Warna, Chemical Reaction Engineering and Reactor Technology, CRC Press, 2010.
[37] H. Kierzkowska-Pawlak, Determination of kinetics in gas-liquid reaction systems. An overview, Ecol. Chem. Eng. S 19 (2012) 175–196.
[38] H.T.H. Kimweri, Enhancement of Gas-Liquid Mass Transfer in Hydrometallurgical Leaching Systems, University of British Columbia, 2001.
[39] M. DÍAZ, A. VEGA, J. COCA, Correlation for the estimation of gas-liquid diffusivity, Chem. Eng. Commun. 52 (1987) 271–281.
[40] F. Javed, Z. Shamair, A. Hafeez, T. Fazal, R. Aslam, S. Akram, N. Rashid, W. B. Zimmerman, F. Rehman, Conversion of poultry-fat waste to a sustainable feedstock for biodiesel production via microbubble injection of reagent vapor, J. Clean. Prod. (2021), 127525.
[41] R.M. Worden, M.D. Bredwell, Mass-transfer properties of microbubbles. 2. Analysis using a dynamic model, Biotechnol. Prog. 14 (1998) 39–46.
[42] N.B. Nakkash, N. Al-Habobi, H.M. Hamodee, Simulation of Batch Reactive Distillation For Methyl Acetate Production, Spring National Meeting AIChE, 2010.
[43] B. Torabi, E. Ameri, Methyl acetate production by coupled esterification-reaction process using synthesized cross-linked PVA/silica nanocomposite membranes, Chem. Eng. J. 288 (2016) 461–472.
[44] C. Rohde, R. Marr, M. Siebenhofer, Investigation of methyl acetate production by reactive extraction, in: Proceedings of the AIChE Annual Meeting, 2004, pp. 5113–5118.

[45] P. Verma, K. Kaur, R.K. Wanchoo, A.P. Toor, Esterification of acetic acid to methyl acetate using activated TiO2 under UV light irradiation at ambient temperature, J. Photochem. Photobiol. A Chemistry 336 (2017) 170–175.

[46] Z. Khan, F. Javed, Z. Shamair, A. Hafeez, T. Fazal, A. Aslam, W.B. Zimmerman, F. Rehman, Current developments in esterification reaction: a review on process and parameters, J. Ind. Eng. Chem. (2021).

[47] W.B. Zimmerman, M.K. Al-Mashhadani, H.H. Bandulasena, Evaporation dynamics of microbubbles, Chem. Eng. Sci. 101 (2013) 865–877.